Generalized conductivity model for polar semiconductors at terahertz frequencies

J. Lloyd-Hughes[a)]
Department of Physics, Clarendon Laboratory, University of Oxford, Parks Road, Oxford OX1 3PU, United Kingdom

A theoretical framework is presented that calculates the conductivity of polar semiconductors at terahertz frequencies without resorting to phenomenological fit parameters, using an expression derived from the Boltzmann transport equation. The time-dependent photoconductivity of InAs and the temperature dependent conductivity of n-doped GaAs are found experimentally by terahertz time-domain spectroscopy. The observed deviation from the Drude-Lorentz conductivity in these model systems is accounted for by this approach, which calculates the energy-dependent electron scattering time. © 2012 American Institute of Physics. [http://dx.doi.org/10.1063/1.3695161]

Time-domain spectroscopy enables the optical properties of a material to be determined in the terahertz and mid-infrared frequency range[1–3] by linking the measured transmission (or reflection) to the complex conductivity $\tilde{\sigma}(\omega) = \sigma_1 + i\sigma_2$. To first order the frequency-dependent conductivity of metals and semiconductors is described by the Drude-Lorentz approach, in which an electron-hole plasma is treated as a non-interacting gas. The complex conductivity is given by

$$\tilde{\sigma}(\omega) = \frac{Ne^2}{m^*}\frac{\tau}{1 - i\omega\tau}, \qquad (1)$$

where N is the density of electrons in a parabolic band with effective mass m^*. Carriers undergo collisions that randomize their momentum in a time τ that is assumed to be independent of their energy E. Optical-pump, terahertz-probe spectroscopy[1–3] allows τ to be determined at different times (and therefore N) after photoexcitation, as has been reported theoretically[4] and experimentally[5] for GaAs.

While the Drude conductivity is adequate to model the intraband conductivity of some metals and semiconductors,[1–3] it often fails as the electron scattering rate is in general energy dependent, and bands are parabolic only close to extrema. In bulk n-type and p-type silicon at room temperature, the Drude model was found to predict a larger imaginary part of the conductivity than measured experimentally.[6,7] An energy dependent scattering time $\tau(E)$ was invoked to explain these results, taking $\tau(E) \propto E^{-1/2}$ for acoustic phonon scattering and $\tau(E) \propto E^{3/2}$ for impurity scattering.[6] The Cole-Cole and Cole-Davidson extensions to the Drude model have also been utilized to account for the conductivity of extrinsic electrons in bulk ZnO (Ref. 8) and photoexcited electrons in bulk semi-insulating and low-temperature grown GaAs.[5,9] In these models, the denominator of Eq. (1) is altered using two exponents, which act as additional fit parameters that enable an energy dependent τ to be included phenomenologically. The localization of charge carriers within nanoparticles has also been invoked to account for non-Drude conductivity, and a recent review of this topic can be found in Ref. 3.

In this article, a straightforward theoretical framework is expounded that enables the influence of an energy-dependent electron scattering time to be included in calculations of the optical conductivity spectra of polar semiconductors. This microscopic approach, based on the semi-classical Boltzmann transport equation, calculates the scattering rate directly from theory rather than taking it as a phenomenological fit parameter. In order to demonstrate the versatility of this approach, an investigation is reported into two model systems: (i) the temperature-dependent conductivity at terahertz frequencies of GaAs epilayers and (ii) the time-dependent photoconductivity of InAs. At room temperature in both cases, the conductivity deviates from that predicted by the Drude-Lorentz model in a way that is accounted for by the Boltzmann conductivity model.

In the relaxation time approximation, the rate of change of the electron distribution function under an external perturbation (such as an electric field) is assumed to be inversely proportional to the scattering time τ. The Boltzmann transport equation in this approximation[10] can be used to derive the frequency dependent conductivity $\tilde{\sigma}(\omega)$ as

$$\tilde{\sigma}(\omega) = \frac{2\sqrt{2m^*}e^2}{3\pi^2\hbar^3}\int_E \frac{\tau(E)E^{3/2}}{1 - i\tau(E)\omega}\left(-\frac{\partial f_0}{\partial E}\right)\mathrm{d}E, \qquad (2)$$

where the Fermi-Dirac function $f_0(E)$ is evaluated at a chemical potential μ. A calculation at each temperature determined μ from the requirement that $N = \int_0^\infty f_0(E)g(E)\mathrm{d}E$, where $g(E)$ is the electronic density of states. In the derivation of Eq. (2), the material was assumed to be isotropic and to have a response that was linear in the applied electric field. Electrons were assumed to have a parabolic energy dispersion E, effective mass m^*, and momentum scattering time $\tau(E)$ (calculated as described below). In the limit of zero temperature, the substitutions $-\partial f_0/\partial E \to \delta(E - \mu)$ and $\mu \to \hbar^2(3\pi^2n)^{2/3}/(2m^*)$ in Eq. (2) produce the Drude conductivity of Eq. (1), and the relevant scattering time is that for electrons at the Fermi surface, $\tau(\mu)$. Equation (1) is also recovered when the scattering time is not a function of energy. The conductivity expression in Eq. (2) was found to be consistent with causality by calculating σ_2 from σ_1 (and vice-versa) using the Kramers-Kronig relations.

a)Electronic mail: james.lloyd-hughes@physics.ox.ac.uk.

In heavily doped polar semiconductors, electrons scatter principally with LO phonons, other electrons, and impurities. The energy dependent momentum scattering time $\tau(E)$ was calculated including these mechanisms using the expressions described in detail in Refs. [11] and [12]. The scattering rate with LO phonons of angular frequency ω_{LO} was calculated assuming the static screened Coulomb potential [Eq. (3.156) of Ref. [11]]. Scattering by collective excitations (plasmons) was assumed to have the same form,[13] and the single particle electron-electron rate was calculated using fast electrons.[11] Parameters for InAs and GaAs were taken from Ref. [14].

The calculated $\tau(E)$ is shown by the solid lines in Fig. 1(a) for n-type GaAs ($N = 9.0 \times 10^{17}$ cm^{-3}) at a temperature $T = 7$ K (top) and $T = 295$ K (bottom). At low temperature, the Fermi-Dirac distribution is narrow, as indicated by its derivative $-\partial f_0/\partial E$ (dashed lines), and only electrons close to the chemical potential (49 meV) can contribute to the conductivity. In contrast at room temperature, $-\partial f_0/\partial E$ is broad, indicating that electrons over a large range of energies can take part in transport. Above the LO-phonon energy (36 meV) and plasmon energy (40 meV), $\tau(E)$ is reduced by the emission of a phonon or plasmon. Figure 1(b) illustrates $\tau(E)$ for InAs ($\hbar\omega_{LO} = 30$ meV) at electron densities of $N_1 = 1.4 \times 10^{16}$ cm^{-3} and $N_2 = 3.9 \times 10^{16}$ cm^{-3}. The value of $\tau(E)$ is reduced at higher electron density mainly by additional electron-plasmon scattering.

The dielectric function of a 500 nm thick, 1×10^{18} cm^{-3} GaAs epilayer[15] was measured by terahertz time-domain transmission spectroscopy[1–3] and can be written $\tilde{\epsilon} = \tilde{\epsilon}_l + i\tilde{\sigma}/\omega\epsilon_0$. The lattice contribution $\tilde{\epsilon}_l(\omega)$ originates from interband transitions and TO-phonons, while $\tilde{\sigma}$ arises from free charges. The temperature dependence of $\tilde{\epsilon}_l$ was obtained from a separate measurement of a semi-insulating GaAs substrate. In Figure 2(a), the measured conductivity of the GaAs epilayer is plotted at $T = 7$ K (crosses) and $T = 295$ K (circles). A fit to the low temperature conductivity σ_1 using the Drude-Lorentz model (Eq. (1)) is in good agreement with experiment when $N = 9.0 \times 10^{17}$ cm^{-3} and $\tau = 95$ fs (fit: solid lines, experiment: crosses). At room temperature (295 K), the experimental σ_1 (circles) can be well described by the Drude-Lorentz model (dashed-dotted lines, $N = 9.0 \times 10^{17}$ cm^{-3}

FIG. 2. (a) Real (σ_1) and imaginary (σ_2) parts of the electronic conductivity of an n-type GaAs epilayer at $T = 7$ K (crosses) and $T = 295$ K (circles). The solid and dashed-dotted lines indicate fits to experiment at low and high temperature using the Drude-Lorentz model. The dashed line shows Eq. (2) at $T = 295$ K for $N = 1.0 \times 10^{18}$ cm^{-3}. (b) Frequency dependence of $\sigma_2/\omega\sigma_1$ at 7 K from experiment (crosses) and from Eq. (2) (solid line). The circles and dashed lines show experiment and calculation at 295 K. (c) Temperature dependence of $\sigma_2/\omega\sigma_1$ at 2 THz from experiment (squares) and calculation (solid line). The dashed line shows $\tau \propto T^{-3/2}$ for LO-phonon scattering.

and $\tau = 88$ fs), but the modelled values of σ_2 are significantly higher than observed. In contrast, the calculated conductivity using Eq. (2) (dashed lines) agrees well with σ_1 and deviates from σ_2 only at frequencies above 1 THz.

The extent of the experimental and theoretical deviation from the Drude prediction can be examined by plotting $\sigma_2/\omega\sigma_1$, where for the Drude model $\tau = \sigma_2/\omega\sigma_1$ is independent of frequency.[16,17] The frequency dependence of $\sigma_2/\omega\sigma_1$ is reported in Fig. 2(b). At 7 K, this function is frequency independent because of the sharpness of the Fermi-Dirac distribution, and the calculated and measured values are in close agreement. As the temperature is raised, the simulated $\sigma_2/\omega\sigma_1$ becomes a function of frequency, with a notable decrease towards higher frequency. This is a consequence of the broadening of the electron distribution function to include electrons with different scattering times $\tau(E)$. The disagreement between the model and experiment suggests that τ may depend more significantly on energy than in Fig. 1(a). This may be a consequence of the simplified scattering mechanisms used to calculate $\tau(E)$. At a doping level of 1×10^{18} cm^{-3} (plasma frequency $\omega_p/2\pi = 10$ THz), the scattering of electrons in GaAs by polar optical phonons should be considered using a time-dependent potential that describes the interaction with coupled plasmon-like and phonon-like modes,[11,18] rather than the static model employed herein.

The temperature dependence of the mobility is often used to examine the electron scattering mechanism that dominates transport. Since the GaAs epilayer is heavily doped, no carrier freeze-out occurs at low temperature, as Fig. 2(c) indicates using the temperature dependence of $\sigma_2/\omega\sigma_1$ at $\omega/2\pi = 2.0$ THz. As temperature increases, $\sigma_2/\omega\sigma_1$ rises to 100 fs at 100 K, before reducing at higher temperatures to 40 fs at 295 K. In comparison, lightly doped GaAs exhibits $\tau = 165$–300 fs at room temperature.[19,20] At high temperatures, $\sigma_2/\omega\sigma_1$ scales in proportion to $T^{-3/2}$ [dashed line in Fig. 2(c)], indicating that an LO-phonon mediated scattering mechanism dominates the conductivity.[12]
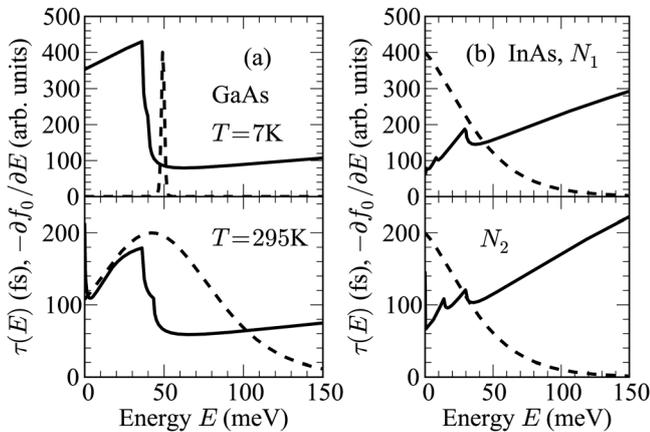

FIG. 1. (a) Calculated dependence of the scattering time τ (solid lines) and $-\partial f_0/\partial E$ (dashed lines) upon the electron energy E for GaAs at $T = 7$ K and $T = 295$ K, with $N = 9 \times 10^{17}$ cm^{-3}. (b) As (a), but for InAs at room temperature at electron densities $N_1 = 1.4 \times 10^{16}$ cm^{-3} and $N_2 = 3.9 \times 10^{16}$ cm^{-3}.
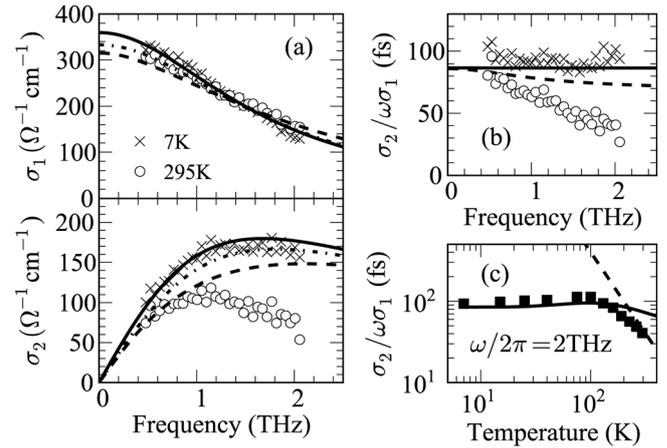
In Fig. 3, the time-resolved photoconductivity[1–3] $\Delta\sigma$ of an InAs epilayer[21] is reported. The sample was photoexcited by 50 fs pulses at 800 nm (1.55 eV), 1.2 eV above the direct bandgap (0.35 eV), producing carriers in the Γ, L, and X-valleys. The photoconductivity exhibits a slow rise over 15 ps, as demonstrated by the real part of the photoconductivity $\Delta\sigma_1$ at 1 THz [circles in Fig. 3(a)]. This can be attributed to the energetic relaxation of hot electrons from high in the bandstructure to the Γ-valley minimum, where electrons contribute more significantly to the photoconductivity because of their substantially smaller effective mass.[22,23] The solid line indicates the calculated photoconductivity using Eq. (2) assuming that $N \propto 1 - e^{-t/\tau_\Gamma}$. The obtained rise time $\tau_\Gamma = 3.8$ ps is comparable to that of hot electrons in GaAs (Ref. 22) and InGaAs,[23] where $\tau_\Gamma = 2-3$ ps, indicating that electrons in InAs have a comparable energy relaxation rate.

The frequency dependence of the photoconductivity at $t = 6.8$ ps after photoexcitation is shown in Fig. 3(b). As for extrinsic electrons in GaAs, the experimental conductivity (points) cannot be modeled well by the Drude-Lorentz expression (solid lines). Examining the frequency dependence of $\Delta\sigma_2/\omega\Delta\sigma_1$ in Fig. 3(c) yields qualitative agreement between calculation (lines) and experiment (points) at $t = 1.5$ ps and $t = 13.5$ ps, corresponding to the carrier densities in Fig. 1(b). The mean scattering time decreases at later times after photoexcitation as the electron density close to the minimum of the Γ valley increases. This is further illustrated in Fig. 3(d) by $\Delta\sigma_2/\omega\Delta\sigma_1$ evaluated at 1 THz from calculation (line) and experiment (circles). The assumption of parabolic bands and the neglection of scattering with coupled phonon-plasmon modes may account for the discrepancy between the model and experiment, however the only free parameter is the electron density, and the agreement is fairly good.

The extended Drude model[16,24] has been extensively applied to the visible and infrared conductivity of metals and superconductors and is applicable for Fermi liquids (when electron-electron interactions are strong), and also when the effective mass is energy dependent. In this approach, the single-particle effective mass m^* in Eq. (1) is replaced by a frequency-dependent function $m^{**}(\omega) = m^*[1 + \lambda(\omega)]$, and the energy-independent scattering time τ is replaced by a photon frequency dependent function $\tau^*(\omega)$. The effective mass renormalization factor $1 + \lambda(\omega)$ can be determined from experiment using $m^{**}(\omega) = -Ne^2\mathrm{Im}[1/\sigma]/\omega$ if the electron density N is known.[16,24] Following this procedure, we find that $m^{**}(\omega)/m^* = 1 + \lambda(\omega)$ is frequency independent and equal to unity within experimental error (e.g., for photoexcited InAs $m^{**}/m^* = 0.97 \pm 0.1$, and for heavily doped GaAs $m^{**}/m^* = 0.95 \pm 0.1$). This provides support for the above assumption of parabolic energy bands.

In summary, a formalism was presented that allows the complex conductivity of polar semiconductors to be calculated at terahertz frequencies by including the energy dependence of the scattering rate. The generalized conductivity reduces to the Drude model in the limit of zero temperature or an energy independent scattering rate. Terahertz time-domain spectroscopy was used to determine the conductivity of heavily doped GaAs and the photoconductivity of InAs, which were semi-quantitatively accounted for by the generalized conductivity model.
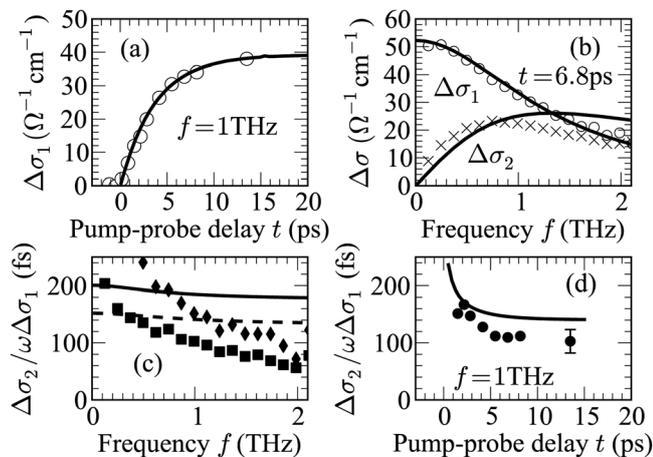
FIG. 3. (a) Real part of photoconductivity of InAs $\Delta\sigma_1$ (at a frequency $f = 1.0$ THz) at different pump-probe delay times t from experiment (circles) and calculation (solid line). (b) $\Delta\sigma_1$ (circles) and $\Delta\sigma_2$ at $t = 6.8$ ps (crosses), and fit using the Drude-Lorentz model (solid lines). (c) σ_2/σ_1 at $t = 1.5$ ps (diamonds) and $t = 13.5$ ps (squares) from experiment. The solid and dashed lines show the calculated values at the same delay times. (d) $\sigma_2/\omega\sigma_1$ at $f = 1$ THz from experiment (circles) and model (solid line) as a function of t.

[1] C. A. Schmuttenmaer, Chem. Rev. **104**, 1759 (2004).
[2] P. U. Jepsen, D. G. Cooke, and M. Koch, Laser Photonics Rev. **5**, 124 (2011).
[3] R. Ulbricht, E. Hendry, J. Shan, T. F. Heinz, and M. Bonn, Rev. Mod. Phys. **83**, 543 (2011).
[4] A. S. Vengurlekar and S. S. Jha, Phys. Rev. B **43**, 12454 (1991).
[5] M. C. Beard, G. M. Turner, and C. A. Schmuttenmaer, Phys. Rev. B **62**, 15764 (2000).
[6] M. van Exter and D. Grischkowsky, Phys. Rev. B **41**, 12140 (1990).
[7] T.-I. Jeon and D. Grischkowsky, Phys. Rev. Lett. **78**, 1106 (1997).
[8] J. B. Baxter and C. A. Schmuttenmaer, Phys. Rev. B **80**, 235205 (2009).
[9] M. C. Beard, G. M. Turner, and C. A. Schmuttenmaer, J. Appl. Phys. **90**, 5915 (2001).
[10] G. Grosso and G. Parravicini, *Solid State Physics* (Academic, New York, 2000).
[11] B. K. Ridley, *Quantum Processes in Semiconductors*, 4th ed. (Oxford University Press, New York, 2004).
[12] P. Y. Yu and M. Cardona, *Fundamentals of Semiconductors*, 3rd ed. (Springer, Berlin, 2003).
[13] K. Tomizawa, *Numerical Simulation of Submicron Semiconductor Devices*, 1st ed. (Artech House, London, 1993).
[14] I. Vurgaftman, J. R. Meyer, and L. R. Ram-Mohan, J. Appl. Phys. **89**, 5815 (2001).
[15] J. Lloyd-Hughes, Y. L. Delley, G. Scalari, M. Fischer, V. Liverini, M. Beck, and J. Faist, J. Appl. Phys. **106**, 093104 (2009).
[16] D. N. Basov and T. Timusk, Rev. Mod. Phys. **77**, 721 (2005).
[17] J. Lloyd-Hughes, S. K. E. Merchant, L. Sirbu, I. M. Tiginyanu, and M. B. Johnston, Phys. Rev. B **78**, 085320 (2008).
[18] R. Huber, C. Kübler, S. Tubel, A. Leitenstorfer, Q. T. Vu, H. Haug, F. Kohler, and M. C. Amann, Phys. Rev. Lett. **94**, 027401 (2005).
[19] G. E. Stillman, C. M. Wolfe, and J. O. Dimmock, J. Phys. Chem. Solids **31**, 1199 (1970).
[20] N. Katzenellenbogen and D. Grischkowsky, Appl. Phys. Lett. **61**, 840 (1992).
[21] M. B. Johnston, D. M. Whittaker, A. Dowd, A. G. Davies, E. H. Linfield, X. Li, and D. A. Ritchie, Opt. Lett. **27**, 1935 (2002).
[22] M. C. Nuss, D. H. Auston, and F. Capasso, Phys. Rev. Lett. **58**, 2355 (1987).
[23] S. E. Ralph, Y. Chen, J. Woodall, and D. McInturff, Phys. Rev. B **54**, 5568 (1996).
[24] W. Gotze and P. Wolfle, Phys. Rev. B **6**, 1226 (1972).